ARTICLE
Journal of Cellular Biochemistry 112:1286–1294 (2011)

Journal of Cellular Biochemistry

# Survivin (*BIRC5*) Cell Cycle Computational Network in Human No-Tumor Hepatitis/Cirrhosis and Hepatocellular Carcinoma Transformation

Lin Wang,[1*] Juxiang Huang,[1] Minghu Jiang,[2] and Lingjun Sun[1]

[1] *Biomedical Center, School of Electronic Engineering, Beijing University of Posts and Telecommunications, Beijing, 100876, China*

[2] *Lab of Computational Linguistics, School of Humanities and Social Sciences, Tsinghua Univ., Beijing, 100084, China*

## ABSTRACT

Survivin (*BIRC5*) relationship with tumor is presented in several papers. However, how the molecular network and interpretation concerning *BIRC5* cell cycle between no-tumor hepatitis/cirrhosis and hepatocellular carcinoma (HCC) remains to be elucidated. Here, we constructed and analyzed significant higher expression gene *BIRC5* activated and inhibited cell cycle network from HCC versus no-tumor hepatitis/cirrhosis pateints (viral infection HCV or HBV) in GEO Dataset by combination of gene regulatory network inference method based on linear programming and decomposition procedure with the CapitalBio MAS 3.0 software based on the integration of public databases including Gene Ontology, KEGG, BioCarta, GenMapp, Intact, UniGene, OMIM, etc. Compared the same and different activated and inhibited *BIRC5* network with GO analysis between no-tumor hepatitis/cirrhosis and HCC, our result showed *BIRC5* cell cycle network weaker transcription factor activity in both no-tumor hepatitis/cirrhosis and HCC (1); stronger nucleus protein binding but weaker cytoplasm protein binding in no-tumor hepatitis/cirrhosis (2); stronger cytoplasm protein phosphatase binding but weaker ubiquitin-protein ligase activity in HCC (3). Therefore, we inferred *BIRC5* cell cycle module less transcription from RNA polymerase II promoter in both no-tumor hepatitis/cirrhosis and HCC (4). We deduced *BIRC5* cell cycle module different from more mitosis but less complex-dependent proteasomal ubiquitin-dependent protein catabolism as a result increasing cell division and cell numbers in no-tumor hepatitis/cirrhosis to more protein amino acid autophosphorylation but less negative regulation of ubiquitin ligase activity during mitotic cell cycle as a result increasing growth and cell volume in HCC (5). J. Cell. Biochem. 112: 1286–1294, 2011. 

**KEY WORDS:** SURVIVIN (*BIRC5*) COMPUTATIONAL NETWORK; CELL CYCLE; HUMAN HEPATOCELLULAR CARCINOMA; NO-TUMOR HEPATITIS/CIRRHOSIS

## INTRODUCTION

Survivin (*BIRC5*) is one of genes we identified as high expression in 25 HCC versus 25 no-tumor hepatitis/cirrhosis. We data-mines *BIRC5* roles in cellular component, molecular function, biological process, KEGG, GenMAPP, BioCarta, and disease from the CapitalBio MAS 3.0 software. GO result illustrates that *BIRC5* cellular component localizes in pericentric region, intracellular, nucleus, chromosome, nucleolus, cytoplasm, centriole, cytosol, spindle microtubule, cytoplasmic microtubule, midbody, interphase microtubule organizing center, protein complex, and molecular function comprises microtubule binding, zinc ion binding, protein homodimerization activity, caspase inhibitor activity, metal ion binding, protein heterodimerization activity, cofactor binding, chaperone binding, and biological process contains G2/M transition of mitotic cell cycle, cytokinesis, apoptosis, anti-apoptosis, cell cycle, mitosis, protein complex localization, positive regulation of exit from mitosis, spindle checkpoint, negative regulation of caspase activity, positive regulation of progression through mitotic cell cycle, establishment of chromosome localization. KEGG analysis shows that *BIRC5* is related to colorectal cancer. GenMAPP analysis shows that *BIRC5* is related to hs_il-3_netpath_15. BioCarta

Lin Wang, Juxiang Huang, and Minghu Jiang were equally contributed to this work.

Grant sponsor: National Natural Science Foundation in China; Grant number: 60871100.

*Correspondence to: Lin Wang, Biomedical Center, School of Electronics Engineering, Beijing University of Posts and Telecommunications, Beijing, 100876, China E-mail: wanglin98@tsinghua.org.cn

Received 19 September 2010; Accepted 11 January 2011 • DOI 10.1002/jcb.23030 • © 2011 Wiley-Liss, Inc.
Published online 10 February 2011 in Wiley Online Library (wileyonlinelibrary.com).

involves b-cell survival pathway. Disease analysis demonstrates that *BIRC5* participates in maple syrup urine disease, metabolic diseases, the organic acidemias an overview. Studying on *BIRC5* relationship with tumor is presented in several papers [Okada et al., 2001; Andersen and Thor, 2002; Sun et al., 2006; Aqui and Vonderheide, 2008; Xia et al., 2008; Guha and Altieri, 2009; Konduri et al., 2009]. However, the distinct molecular network and interpretation concerning *BIRC5* cell cycle during no-tumor hepatitis/cirrhosis and hepatocellular carcinoma (HCC) transformation remains to be elucidated.

HCC is one of the most common causes of cancer-related death. So to develop novel drugs in HCC has become a challenge for biologists. Here, we constructed and analyzed significant higher expression gene *BIRC5* activated and inhibited cell cycle network from HCC versus no-tumor hepatitis/cirrhosis pateints (viral infection HCV or HBV) in GEO Dataset by combination of gene regulatory network inference method based on linear programming and decomposition procedure with the CapitalBio MAS 3.0 software based on the integration of public databases including Gene Ontology, KEGG, BioCarta, GenMapp, Intact, UniGene, OMIM, etc. The mechanisms that shut off a signal are as important as the mechanisms that turn it on. GRNInfer tool [Wang et al., 2006] can identified molecular activation and inhibition relationships based on a novel mathematic method called GNR (Gene Network Reconstruction tool) using linear programming and a decomposition procedure for inferring gene networks. The method theoretically ensures the derivation of the most consistent network structure with respect to all of the datasets, thereby not only significantly alleviating the problem of data scarcity but also remarkably improving the reconstruction reliability.

In this study, our result showed *BIRC5* cell cycle network weaker transcription factor activity in both no-tumor hepatitis/cirrhosis and HCC (1); stronger nucleus protein binding but weaker cytoplasm protein binding in no-tumor hepatitis/cirrhosis (2); stronger cytoplasm protein phosphatase binding but weaker ubiquitin-protein ligase activity in HCC (3). Therefore, we inferred *BIRC5* cell cycle module less transcription from RNA polymerase II promoter in both no-tumor hepatitis/cirrhosis and HCC (4). We deduced *BIRC5* cell cycle module different from more mitosis but less complex-dependent proteasomal ubiquitin-dependent protein catabolism as a result increasing cell division and cell numbers in no-tumor hepatitis/cirrhosis to more protein amino acid autophosphorylation but less negative regulation of ubiquitin ligase activity during mitotic cell cycle as a result increasing growth and cell volume in HCC (5).

## MATERIALS AND METHODS

### MICROARRAY DATA

We used microarrays containing 6,144 genes from 25 no-tumor hepatitis/cirrhosis and 25 HCC patients in the same GEO Dataset GSE10140-10141 (http://www.ncbi.nlm.nih.gov/geo/query/acc.cgi?acc= GSE10140, http://www.ncbi.nlm.nih.gov/geo/query/acc.cgi?acc=GSE10141) [Hoshida et al., 2008]. We preprocessed raw microarray data as log2.

### GENE SELECTION ALGORITHMS

Potential HCC molecular markers were identified using significant analysis of microarrays (SAM). SAM is a statistical technique for finding significant genes in a set of microarray experiments. The input to SAM is gene expression measurements from a set of microarray experiments, as well as a response variable from each experiment. The response variable might be a grouping like untreated, treated, and so on. SAM computes a statistic $d_i$ for each gene *i*, measures the strength of the relationship between gene expression and the response variable. It uses repeated permutations of the data to determine if the expression of any genes is significantly related to the response. The cutoff for significance is determined by a tuning parameter delta, chosen by the user based on the false positive rate. We normalized data by log2, selected two classes paired and minimum fold change $\geq$2, and chose the significant (high expression genes of HCC compared with no-tumor hepatitis/cirrhosis) genes under the false-discovery rate and q-value were 0%. The q-value (invented by John Storey [Storey, 2002]) is like the well-known *P*-value, but adapted to multiple-testing situations.

### UNSUPERVISED CLUSTERING

Two hundred and twenty five significant higher expression genes from no-tumor hepatitis/cirrhosis versus HCC was done unsupervised clustering using cluster 3.0 (http://bonsai.ims.tokyo.ac.jp/~mdehoon/software/cluster). We chose average linkage of hierarchical clustering, and the steps are as follows: step 1, loading and filtering data; step 2, normalizing for adjusting data; step 3, choosing similarity methods, measuring the distance/similarity; step 4, choosing hierarchical Cluster; and step 5, doing TreeView.

### MOLECULE ANNOTATION SYSTEM (MAS)

MAS is a web-based software toolkit for a whole data mining and function annotation solution to extract and analyze biological molecules relationships from public databases of biological molecules and signification. MAS uses relational database of biological networks created from millions of individually modeled relationships between genes, proteins, complexes, cells, disease, and tissues. MAS allows a view on your data, integrated in biological networks according to different kinds of biological context. This unique feature results from multiple lines of evidences which are integrated in MASCORE. MAS helps to understand relationship of gene expression data through the given molecular symbols list, and provides thorough, unbiased, and visible results.

The primary databases of MAS integrated various well-known biological resources such as Genbank, EMBL, SwissProt, Gene Ontology, KEGG, BioCarta, GenMapp, mirBase, EPD, HPRD, MIND, BIND, Intact, TRANSFAC, UniGene, dbSNP, OMIM, InterPro, HUGO, MGI, and RGD. MAS offers various query entries and graphics result. The system represents an alternative approach to mining and catching on biological signification for high-throughput array data.

### NETWORK ESTABLISHMENT OF CANDIDATE GENES

The entire network was constructed using GRNInfer [Wang et al., 2006] and GVedit tools (http://www.graphviz.org/About.php). GRNInfer is a novel mathematic method called GNR (Gene Network

Reconstruction tool) based on linear programming and a decomposition procedure for inferring gene networks. The method theoretically ensures the derivation of the most consistent network structure with respect to all of the datasets, thereby not only significantly alleviating the problem of data scarcity but also remarkably improving the reconstruction reliability. The following equation (1) represents all of the possible networks for the same dataset.

$$J = (X'\text{-}A)U\Lambda^{-1}V^{T} + YV^{T} = \hat{J} + YV^{T} \quad (1)$$

where $J = (J_{ij})_{n\times n} = \partial f(x)/\partial x$ is an $n \times n$ Jacobian matrix or connectivity matrix, $X = (x'(t_1),\ldots,x(t_m))$, $A = (a(t_1),\ldots,a(t_m)$ and $X' = (x'(t_1),\ldots,x'(t_m))$ are all $n \times m$ matrices with $x'_i(t_j) = [x_i(t_j + 1) - x_i(t_j)]/[t_{j+1} - t_j]$ for $i = 1,\ldots,n$; $j = 1,\ldots,m$. $X(t) = (x_1(t),\ldots,x_n(t))^T \in R_n$, $a = (a_1\ldots,a_n)^T \in R_n$, $x_i(t)$ is the expression level (mRNA concentrations) of gene i at time instance t. $y = (y_{ij})$ is an $n \times n$ matrix, where $y_{ij}$ is zero if $ej \neq 0$ and is otherwise an arbitrary scalar coefficient. $\wedge^{-1} = \text{diag}\ (1/e_i)$ and $1/e$ is set to be zero if $e_i = 0$. U is a unitary $m \times n$ matrix of left eigenvectors, $\wedge = \text{diag}\ (e_1,\ldots,e_n)$ is a diagonal $n \times n$ matrix containing the n eigenvalues and $V^T$ is the transpose of a unitary $n \times n$ matrix of right eigenvectors. We established network based on the fold change $\geq 2$ distinguished genes and selected parameters as lambda 0.0 because we used one dataset and tried several thresholds 1, 0.5, 0.1, 0.001, 0.0001, 0.000001, 0.0000001, 0.00000001, 0.000000001. Lambda was a positive parameter, which balanced the matching and sparsity terms in the objective function. Using different thresholds, we could predict various networks with different edge density.

## RESULTS

### IDENTIFICATION OF HCC NOVEL MOLECULAR MARKERS

We normalized data by log2, selected two classes paired and minimum fold change $\geq 2$, and chose the significant (high expression genes of HCC compared with no-tumor hepatitis/cirrhosis) genes under the false-discovery rate and q-value were 0%. We obtained 225 significant high expression molecules (fold change $\geq 2$) from 6,144 genes of 25 HCC versus 25 no-tumor hepatitis/cirrhosis in the same GEO Dataset GSE10140-10141 containing *NEK2*, *NUSAP1*, *CAD*, *DLGAP5*, *LCN2*, *SFRP4*, *RRM2*, *HIST1H3H*, *TAGLN2*, *MYBL2*, *TK1*, *PRCC*, *E2F1*, *ACTN2*, etc., as shown in Table I.

### UNSUPERVISED CLUSTERING

Two hundred and twenty five significant higher expression genes from no-tumor hepatitis/cirrhosis versus HCC was done unsupervised clustering using cluster 3.0. We chose average linkage of hierarchical clustering. Our result showed most control group (no-tumor hepatitis/cirrhosis) clustered together and most experiment group also together. Two group were observed red colors reflecting all the upregulation and no missing data in both no-tumor hepatitis/cirrhosis and HCC, as shown in Figure 1.

### CANDIDATE NOVEL ACTIVATED AND INHIBITED GENES OF *BIRC5* UPSTREAM AND DOWNSTREAM NETWORK IN HUMAN NO-TUMOR HEPATITIS/CIRRHOSIS AND HCC BY GRNInfer

We tried GRNInfer in several thresholds 1, 0.5, 0.1, 0.001, 0.0001, 0.000001, 0.0000001, 0.00000001, 0.000000001. At last we selected threshold 0.000000001 because its result covered *BIRC5* pathway by the CapitalBio MAS 3.0 software from the published data. We identified candidate genes of *BIRC5* upstream and downstream network from our constructed total network between no-tumor hepatitis/cirrhosis and HCC by GRNInfer separately, as shown in Table II.

## DISCUSSION

Our aim is to compare and analyze novel *BIRC5* cell cycle network between no-tumor hepatitis/cirrhosis and HCC transformation for

TABLE I. Abbreviations of 225 Significant High Expression Genes (Fold $\geq 2$) of HCC Compared With Human No-Tumor Hepatitis/Cirrhosis

| Gene | Gene | Gene | Gene | Gene | Gene | Gene | Gene | Gene | Gene |
|---|---|---|---|---|---|---|---|---|---|
| ACTG2 | CAMK1 | CHST1 | DKK1 | GJA5 | KCNQ3 | MAN2A1 | MYBL2 | PAGE4 | RBCK1 |
| ACTN2 | CBX5 | CIAO1 | DLGAP5 | GML | KCTD2 | MAOA | MYCN | PCOLCE2 | RBM34 |
| ADAMDEC1 | CCL20 | CKS1B | E2F1 | GNAZ | KIAA0101 | MAP2 | MYH6 | PHLDA2 | REG1A |
| AFP | CCNA2 | CLIC1 | ECT2 | GNG10 | KIAA0513 | MAP2K6 | MYOM1 | PIGC | REG3A |
| AKR1B10 | CCNB1 | CNTNAP2 | EFNA1 | GPC3 | KIAA0859 | MAP4K4 | NAT9 | PLA2G1B | RFC4 |
| ALDH3A1 | CCNB2 | CORO2A | EIF1AX | GPSM2 | KLHL35 | MAPK3 | NCAPH | PLK4 | RIMS3 |
| ALK | CCNE2 | CPD | ELAVL3 | GRM1 | KLRC3 | MAPT | NEK2 | POLD1 | RNF185 |
| AMELY | CD34 | CRYGA | ENAH | HIST1H2AD | KPNA2 | MCM2 | NFKBIB | PPP1R12B | RNF2 |
| ARHGDIG | CDC2 | CSPG4 | EPHA4 | HIST1H2AG | LAPTM4B | MCM4 | NINJ2 | PRCC | ROBO1 |
| B4GALNT2 | CDC20 | CST6 | ESM1 | HIST1H2BJ | LCN2 | MCM7 | NKX2-5 | PRKCG | RRM2 |
| BAP1 | CDC6 | CSTB | ESPL1 | HIST1H3H | LEF1 | MDK | NOTCH3 | PRKG2 | RRP1B |
| BCAT1 | CDH13 | CSTF2 | EYA1 | HMGB2 | LGALS3 | MELK | NOTCH4 | PROK1 | S100P |
| BIRC5 | CDKN2C | CTHRC1 | F13A1 | HOMER2 | LLGL2 | METAP2 | NQO1 | PRSS1 | SBF1 |
| BLVRA | CDKN3 | CYP17A1 | FGF9 | HOXA5 | LOX | MKRN3 | NR5A1 | PSMC3IP | SCGB1D2 |
| BRCA1 | CEBPA | CYP21A2 | FKBP1B | HOXD4 | LTBP2 | MMP11 | NRXN3 | PTH2R | SCML2 |
| BUB IB | CELSR2 | CYP27B1 | FOLR1 | IGF2BP3 | LTBP3 | MMP9 | NTN1 | PTHLH | SEMA3B |
| C4orf8 | CENPF | CYP51A1 | FOXM1 | IRF5 | LYPD3 | MRPL49 | NUP62 | PTTG1 | SERPINB2 |
| C9orf127 | CHAF1A | DDX10 | GALK1 | ISG20 | MAGI1 | MS4A1 | NUSAP1 | PVRL2 | SFRP4 |
| CAD | CHL1 | DDX11 | GAS7 | ITGA2 | ZNF43 | MS4A2 | OCRL | RAB3B | SFTPA2B |
| ZIC2 | CHRNA4 | DFFB | GDPD5 | KATNB1 | ZWINT | MUTYH | ORC1L | RABGGTA | SLC16A3 |
| ORC6L | TPSD1 | TRAF2 | TRIP13 | TSHB | TSTA3 | TUBG1 | UNG | VDR | XRCC2 |
| TOP2A | TPST2 | TRIM26 | TROAP | TSR1 | TTK | UBE2C | VCAN | WDR1 | YWHAE |
| SLC4A3 | SORT1 | SPINK1 | SQLE | ST6GALNAC2 | STX1A | SULT1C4 | TAGLN2 | TBL3 | TK1 |
| SLC6A12 | SOX2 | SPON2 | SSTR5 | STMN1 | SULT1C2 | SYN2 | TANK | TCAP | TNFRSF9 |
| TP53I11 | | | | | | | | | |

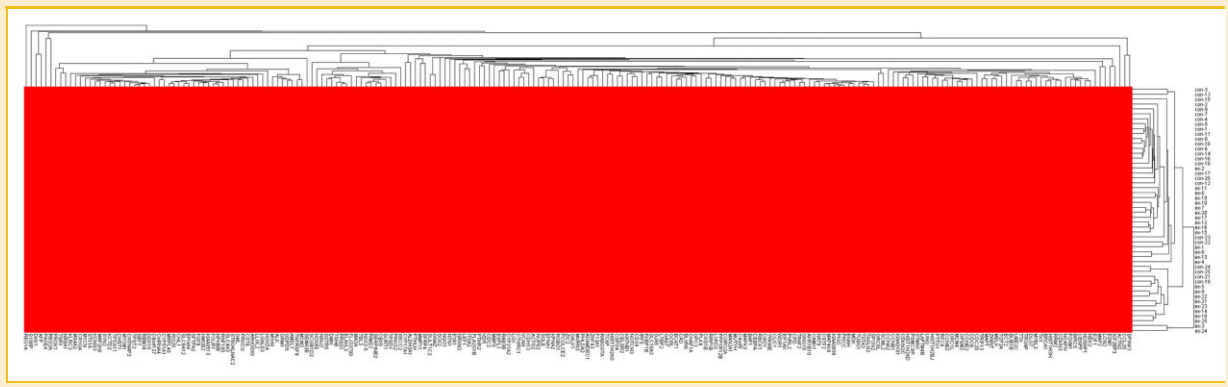

Fig. 1. Unsupervised clustering of 225 significant higher expression genes from no-tumor hepatitis/cirrhosis vs. HCC using cluster 3.0. con 1–25 represents 1–25 human no-tumor hepatitis/cirrhosis patients; ex 1–25 represents 1–25 HCC patients.

TABLE II. Candidate Upstream and Downstream Genes of *BIRC5* Network in Human No-Tumor Hepatitis/Cirrhosis and HCC Transformation by GRNInfer, Respectively

| Control | Experiment |
|---|---|
| *BIRC5* upstream | |
| *NEK2, NUSAP1, CDKN3, DLG7, LCN2, SFRP4, RRM2, TROAP, HIST1H3H, TAGLN2, MYBL2, TK1, PRCC, BRCA1, CENPF, SCML2, TOP2A, SPINK1, MDK, GNG10, FOXM1, TRAF2, SPON2, RAB3B, ECT2, EN AH, PIGC, TTK, CDC20, GPSM2, PLK4, MAPT, VDR, MCM2, CIAO1, XRCC2, MELK, MAP4K4, MAP2, AMELY, CDC6, SEMA3B, TUBG1, KIAA0513, CSTF2, CPD, TNFRSF9, IGF2BP3, NCAPH, YWHAE, SBF1, PVRL2, ORC1L, EIF1AX, GDPD5, GRM1, ARHGDIG, MCM4, LLGL2, BUB1B, GALK1, ACTN2, RBCK1, DDX10, C9orf127, PTTG1, ACTG2, CLIC1, RNF185, CCNA2, LTBP2, SORT1, CDH13, GPC3, ST6GALNAC, CYP21A2, AKR1B10, CEBPA, PRKCG, HIST1H2AG, CST6, MYH6, HOXD4, CAMK1, MUTYH, PSMC3IP, SFTPA2, ALK, CDC2, CD34, NFKBIB, CHST1, NOTCH3, FOLR1, BLVRA, LGALS3, RFC4, MKRN3, CHAF1A, KPNA2, ITGA2, EPHA4, CELSR2, SLC16A3, MAPK3, TPSD1, GJA5, RRP1B, BAP1, CAD, REG3A, ESM1, WDR1, LYPD3, GML, ROBO1, ORC6L, MYCN, AFP, CCL20, CBX5, LEF1, IRF5, ISG20, PRKG2, SLC6A12, REG1A, TPST2, S100P, MAP2K6, CHL1, MMP9, CORO2A, PTHLH, SQLE, PHLDA2, CSPG4, CCNB1, UNG, SULT1C2, MAO A, ZNF43, HOXA5, GAS7, CYP51A1, EYA1, PRSS1, CHRNA4, KATNB1, MAN2A1, OCRL, F13A1, VCAN, STMN1, FLJ33790, EFNA1, PLA2G1B, KCNQ3, PAGE4, CDKN2C, NQO1, KIAA0101, TSHB, KLRC3, DKK1, ESPL1, MRPL49, NKX2-5, PTHR2, NTN1, CTHRC1, TBL3, MMP11, TSR1, ADAMDEC1, MS4A2, SCGB1D2, PCOLCE2, NUP62, NINJ2, LAPTM4B, DMN, RABGGTA, SOX2, SSTR5, NRXN3, BIRC5*<br><br>*BIRC5* downstream | *NUSAP1, CDKN3, DLG7, LCN2, SFRP4, RRM2, TROAP, HIST1H3H, TAGLN2, MYBL2, TK1, PRCC, E2F1, BRCA1, CENPF, SCML2, TOP2A, SPINK1, MDK, GNG10, FOXM1, TRAF2, SPON2, RAB3B, ECT2, KIAA0859, ENAH, PIGC, SLC4A3, CDC20, GPSM2, PLK4, TSTA3, MAPT, VDR, MCM2, CIAO1, XRCC2, MELK, MAP4K4, CCNE2, MAP2, AMELY, CDC6, SEMA3B, TUBG1, KIAA0513, CSTF2, TNFRSF9, IGF2BP3, NCAPH, YWHAE, SBF1, PVRL2, ORC1L, EIF1AX, ZWINT, GDPD5, GRM1, ARHGDIG, MCM4, LLGL2, BUB1B, GALK1, ACTN2, RBCK1, DDX10, C9orf127, PTTG1, ACTG2, CLIC1, RNF185, CCNA2, RBM34, SORT1, ZIC2, CDH13, GPC3, ST6GALNAC, CYP21A2, AKR1B10, CEBPA, PRKCG, HIST1H2AG, UBE2C, CCNB2, CST6, NAT9, MYH6, HOXD4, CNTNAP2, MUTYH, PSMC3IP, SFTPA2, ALK, CDC2, CD34, NFKBIB, TP53I11, CHST1, NOTCH3, HMGB2, FOLR1, BLVRA, LGALS3, RFC4, CHAF1A, KPNA2, ITGA2, EPHA4, CELSR2, SLC16A3, GNAZ, KCTD2, MAPK3, TPSD1, GJA5, RRP1B, BAP1, CAD, HIST1H2BJ, PPP1R12B, REG3A, ESM1, WDR1, LYPD3, TRIP13, GML, ROBO1, ORC6L, FGF9, SYN2, MYCN, ELAVL3, AFP, CCL20, CBX5, LEF1, SERPINB2, IRF5, BCAT1, PRKG2, SLC6A12, REG1A, C4orf8, TPST2, S100P, NR5A1, MAP2K6, CHL1, HIST1H2AD, MMP9, CORO2A, PTHLH, SQLE, PHLDA2, CSPG4, CCNB1, CRYGA, STX1A, UNG, SULT1C2, MYOM1, MAOA, ZNF43, FKBP1B, HOXA5, GAS7, CYP51A1, EYA1, PRSS1, CHRNA4, KATNB1, MAN2A1, OCRL, ALDH3A1, F13A1, VCAN, STMN1, FLJ33790, EFNA1, PLA2G1B, KCNQ3, PAGE4, TCAP, CDKN2C, NQO1, KIAA0101, TSHB, KLRC3, DKK1, ESPL1, MRPL49, RIMS3, NKX2-5, PTHR2, NTN1, CTHRC1, TBL3, MMP11, PROK1, TSR1, ADAMDEC1, MS4A2, SCGB1D2, PCOLCE2, NUP62, NINJ2, LAPTM4B, DMN, RABGGTA, LOX, SSTR5, NRXN3, BIRC5* |
| *NEK2, NUSAP1, CDKN3, DLG7, LCN2, SFRP4, RRM2, TROAP, HIST1H3H, TAGLN2, MYBL2, TK1, PRCC, E2F1, BRCA1, CENPF, SCML2, BIRC5, TOP2A, SPINK1, GNG10, FOXM1, TRAF2, SPON2, RAB3B, ECT2, KIAA0859, ENAH, PIGC, SLC4A3, TTK, CDC20, GPSM2, PLK4, TSTA3, MAPT, VDR, MCM2, CIAO1, XRCC2, MELK, MAP4K4, MAP2, AMELY, CDC6, SEMA3B, TUBG1, KIAA0513, CSTF2, CPD, TNFRSF9, IGF2BP3, NCAPH, YWHAE, SBF1, PVRL2, ORC1L, EIF1AX, ZWINT, GDPD5, GRM1, ARHGDIG, MCM4, BUB1B, GALK1, ACTN2, RBCK1, DDX10, C9orf127, PTTG1, ACTG2, CLIC1, RNF185, CCNA2, RBM34, LTBP2, SORT1, CDH13, GPC3, ST6GALNAC, CYP21A2, AKR1B10, CEBPA, PRKCG, HIST1H2AG, UBE2C, CCNB2, CST6, NAT9, MYH6, HOXD4, CAMK1, CNTNAP2, MUTYH, PSMC3IP, SFTPA2, ALK, CDC2, CD34, NFKBIB, TP53I11, HMGB2, FOLR1, BLVRA, LGALS3, RFC4, MKRN3, CHAF1A, KPNA2, ITGA2, EPHA4, CELSR2, SLC16A3, GNAZ, KCTD2, MAPK3, TPSD1, GJA5, RRP1B, BAP1, CAD, HIST1H2BJ, REG3A, ESM1, WDR1, LYPD3, TRIP13, GML, CKS1B, ROBO1, ORC6L, FGF9, SYN2, MYCN, ELAVL3, AFP, CCL20, CBX5, LEF1, SERPINB2, IRF5, ISG20, BCAT1, PRKG2, SLC6A12, REG1A, TPST2, S100P, NR5A1, MAP2K6, CHL1, HIST1H2AD, MMP9, CORO2A, PTHLH, SQLE, PHLDA2, CSPG4, CCNB1, CRYGA, UNG, SULT1C2, MYOM1, MAOA, ZNF43, FKBP1B, HOXA5, GAS7, CYP51A1, EYA1, PRSS1, CHRNA4, MAN2A1, OCRL, ALDH3A1, VCAN, STMN1, FLJ33790, EFNA1, PLA2G1B, KCNQ3, PAGE4, TCAP, CDKN2C, NQO1, CYP17A1, KIAA0101, TSHB, KLRC3, DKK1, ESPL1, MRPL49, RIMS3, PTHR2, NTN1, CTHRC1, TBL3, MMP11, PROK1, TSR1, MS4A2, PCOLCE2, NUP62, NINJ2, LAPTM4B, DMN, RABGGTA, LOX, SOX2, SSTR5, NRXN3* | *NEK2, NUSAP1, DLG7, SFRP4, RRM2, TROAP, HIST1H3H, TAGLN2, MYBL2, TK1, PRCC, E2F1, BRCA1, CENPF, SCML2, BIRC5, TOP2A, SPINK1, MDK, GNG10, FOXM1, TRAF2, SPON2, ECT2, KIAA0859, PIGC, SLC4A3, TTK, CDC20, GPSM2, TSTA3, MAPT, VDR, MCM2, XRCC2, MELK, MAP4K4, CCNE2, MAP2, AMELY, CDC6, SEMA3B, TUBG1, KIAA0513, CSTF2, CPD, TNFRSF9, IGF2BP3, NCAPH, YWHAE, SBF1, PVRL2, ORC1L, EIF1AX, ZWINT, GDPD5, GRM1, ARHGDIG, MCM4, LLGL2, BUB1B, DDX10, C9orf127, PTTG1, ACTG2, CLIC1, RNF185, RBM34, LTBP2, SORT1, ZIC2, CDH13, GPC3, CYP21A2, AKR1B10, CEBPA, PRKCG, HIST1H2AG, UBE2C, CCNB2, CST6, NAT9, MYH6, HOXD4, CAMK1, CNTNAP2, MUTYH, PSMC3IP, SFTPA2, ALK, CDC2, CD34, NFKBIB, CHST1, NOTCH3, HMGB2, FOLR1, LGALS3, RFC4, MKRN3, CHAF1A, KPNA2, ITGA2, EPHA4, CELSR2, SLC16A3, KCTD2, MAPK3, TPSD1, GJA5, RRP1B, BAP1, CAD, HIST1H2BJ, PPP1R12B, REG3A, ESM1, WDR1, LYPD3, TRIP13, GML, CKS1B, ROBO1, ORC6L, SYN2, MYCN, ELAVL3, AFP, CCL20, CBX5, LEF1, SERPINB2, ISG20, BCAT1, PRKG2, SLC6A12, C4orf8, TPST2, S100P, NR5A1, MAP2K6, CHL1, HIST1H2AD, MMP9, CORO2A, PTHLH, SQLE, PHLDA2, CSPG4, CCNB1, CRYGA, STX1A, UNG, SULT1C2, MYOM1, MAOA, ZNF43, HOXA5, GAS7, CYP51A1, EYA1, PRSS1, CHRNA4, KATNB1, MAN2A1, ALDH3A1, F13A1, VCAN, STMN1, EFNA1, KCNQ3, PAGE4, CDKN2C, NQO1, CYP17A1, KIAA0101, TSHB, KLRC3, DKK1, ESPL1, MRPL49, RIMS3, NKX2-5, PTHR2, NTN1, TBL3, MMP11, PROK1, TSR1, ADAMDEC1, MS4A2, SCGB1D2, PCOLCE2, NUP62, NINJ2, DMN, RABGGTA, LOX, SOX2, SSTR5, NRXN3, BIRC5* |

Control: human no-tumor hepatitis/cirrhosis. Experiment: HCC patients.

potential novel markers to prognosis and therapy of HCC. Based on our published other novel molecular network construction and functional comparison from different databases presented in our papers [Huang et al., 2010a,b; Sun et al., 2008, 2009; Wang et al., 2010a,b,c,d; Wang et al., 2009a,b], we constructed and analyzed significant higher expression gene *BIRC5* activated and inhibited cell cycle network from HCC versus no-tumor hepatitis/cirrhosis pateints (viral infection HCV or HBV) in GEO Dataset by combination of gene regulatory network inference method based on linear programming and decomposition procedure with the CapitalBio MAS 3.0 software based on the integration of public databases including Gene Ontology, KEGG, BioCarta, GenMapp, Intact, UniGene, OMIM, etc. We identified the same and different novel activated and inhibited upstream and downstream genes of *BIRC5* cell cycle module between no-tumor hepatitis/cirrhosis and HCC, on the condition that our *BIRC5* network covered *BIRC5* pathway and matched cell cycle enrichment analysis by the CapitalBio MAS 3.0 software from the published data.

To verify whether our 225 identified genes could separate two samples groups (HCC vs. no-tumor tissue), we did average linkage of hierarchical clustering. Our result showed most control group (no-tumor hepatitis/cirrhosis) clustered together and most experiment group (HCC) also together. Two groups were observed red colors reflecting all the upregulation and no missing data in both no-tumor hepatitis/cirrhosis and HCC (Figure 1). Our unsupervised clustering with expression levels of the 225 identified genes could test separation of two samples groups (HCC vs. no-tumor tissue).

To confirm our prediction for covering the published data, we setup *BIRC5* interaction and pathway in HCC using the CapitalBio MAS 3.0 software for standard comparison with our *BIRC5* network. We identified *BIRC5* interaction and pathway from our total established network by inputting 225 significant high expression genes (fold change $\geq$2) to the CapitalBio MAS 3.0 software based on the integration of public databases including Gene Ontology, KEGG, BioCarta, GenMapp, Intact, UniGene, OMIM, etc. *BIRC5* interaction molecules included *CASP3*, *CASP7*, *CASP9*, *INCENP*, *AURKB*, *DIABLO*, *CDCA8*, *CDC2*, *HSP90AA2*, *BIRC5*, *CDK4*, *XIAP*, *XPO1*, *RASA1*, *USF2*, *PPP1CC*, *BIRC6*. *BIRC5* pathway molecules consisted of *NEK2*, *BRCA1*, *TTK*, *CDC20*, *MAPT*, *MAP2*, *TUBG1*, *ESPL1*, *DLGAP5*, *MELK*, *RFC4*, *CKS1B*, *CCNB1*, *MYBL2*, *SERPINB2*, *E2F1*, *TRAF2*, *DFFB*, *GML*, *PHLDA2*, *NTN1*, *SPINK1*, *PTTG1*, *CST6*, *CSTB*, *CDKN2C*, *NFKBIB*, *IRF5*, *MAPK3*, *LEF1*, *MMP9*, *AFP*. By similarity comparison, our high expression molecules of HCC did not contain *BIRC5* interaction proteins, whereas completely covered *BIRC5* pathway proteins.

To establish candidate novel genes of *BIRC5* upstream and downstream network covering *BIRC5* pathway, we tried GRNInfer in several thresholds 1, 0.5, 0.1, 0.001, 0.0001, 0.000001, 0.0000001, 0.00000001, 0.000000001. At last we selected threshold 0.000000001 and set up candidate genes of *BIRC5* network between no-tumor hepatitis/cirrhosis and HCC by GRNInfer (Table II). Our GRNInfer result was verified covering *BIRC5* pathway by the CapitalBio MAS 3.0 software from the published data.

To construct novel *BIRC5* cell cycle module between no-tumor hepatitis/cirrhosis and HCC, respectively, by GRNInfer, our *BIRC5* network need to match cell cycle enrichment analysis. We identified cell cycle enrichment from our total established enrichment results by inputting 225 significant high expression genes (fold change $\geq$2) to the CapitalBio MAS 3.0 software based on the integration of public databases including Gene Ontology, KEGG, BioCarta, GenMapp, Intact, UniGene, OMIM, etc. We data-mined molecules of cell cycle enrichment including *BIRC5*, *NEK2*, *NUSAP1*, *CDKN3*, *DLGAP5*, *CDC20*, *MCM2*, *MCM7*, *CCNE2*, *CDC6*, *ZWINT*, *LLGL2*, *PTTG1*, *CCNA2*, *UBE2C*, *CCNB2*, *CDC2*, *CHAF1A*, *MAPK3*, *CKS1B*, *DDX11*, *CCNB1*, *KATNB1*, *CDKN2C*. Based on cell cycle enrichment, we predicted novel candidate activated and inhibited upstream and downstream network of *BIRC5* cell cycle between no-tumor hepatitis/cirrhosis and HCC by GRNInfer separately, as shown in Figure 2A,B. Studying on cell cycle relationship with tumor is presented in many papers [Fey, 2000; Turovets et al., 2000; Xu et al., 2001; Helt et al., 2002; van der Veen et al., 2002; Adhikari et al., 2003; Dou et al., 2003; Patino-Garcia et al., 2003; Warrener et al., 2003; Braun et al., 2004; Cheng, 2004; Choudhury et al., 2004; Mhawech et al., 2004; Pham et al., 2004; Arlt et al., 2005; Kim et al., 2005; Kuntzen et al., 2005; Schoonjans et al., 2005; Sotillo et al., 2005; Cheung et al., 2008; Schwartz et al., 2008; Xiong et al., 2008; Graf et al., 2009; Liang et al., 2009; Stewart et al., 2009; Zolochevska and Figueiredo, 2009]. However, how the implication concerning *BIRC5* cell cycle network between no-tumor hepatitis/cirrhosis and HCC transformation remains to be elucidated. We further compared and interpret the candidate same and different molecules of *BIRC5* cell cycle module between no-tumor hepatitis/cirrhosis and HCC transformation considering activation and inhibition relationship.

Firstly, we identified the same novel molecules of *BIRC5* cell cycle module in both no-tumor hepatitis/cirrhosis and HCC. The same upstream *NUSAP1*, *CDC20*, *MCM2*, *CDC6*, *PTTG1*, *CDC2*, *CHAF1A*, *MAPK3* inhibited *BIRC5*. The same downstream showed no results in both no-tumor hepatitis/cirrhosis and HCC. In order to interpret molecular mechanism of *BIRC5* cell cycle module between no-tumor hepatitis/cirrhosis and HCC transformation, we analyzed GO of the same activated and inhibited molecules. For example, inhibited *PTTG1* in no-tumor hepatitis/cirrhosis and HCC cellular component localized in nucleus, cytoplasm, cytosol, and molecular function comprised transcription factor activity, cysteine protease inhibitor activity, protein binding, SH3 domain binding, and biological process was involved in DNA repair, transcription from RNA polymerase II promoter, response to DNA damage stimulus, cell cycle, chromosome segregation, mitosis, spermatogenesis, chromosome organization and biogenesis, cell division. Our result showed the same molecular network of *BIRC5* cell cycle module weaker transcription factor activity in both no-tumor hepatitis/cirrhosis and HCC. Therefore, we deduced *BIRC5* cell cycle module less transcription from RNA polymerase II promoter as common characteristics in both no-tumor hepatitis/cirrhosis and HCC.

Secondly, we identified the different novel molecules of *BIRC5* cell cycle module in no-tumor hepatitis/cirrhosis compared with HCC. The different upstream *CDKN3*, *LLGL2*, *CCNB1*, *CDKN2C* activated *BIRC5*, and *NEK2*, *CCNA2*, *KATNB1* inhibited *BIRC5*. The different downstream *BIRC5* activated *CDKN3*, *ZWINT*, *CCNA2*,

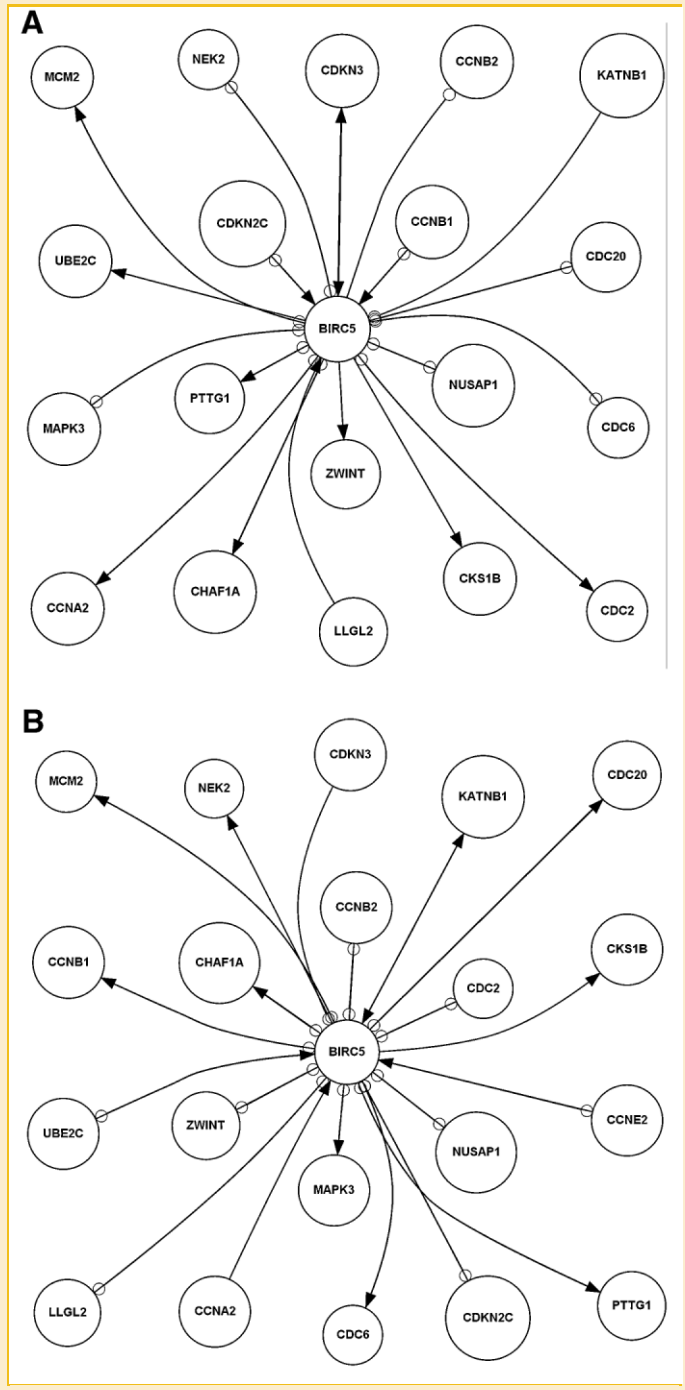


Fig. 2. A: Candidate activated and inhibited upstream and downstream network of *BIRC5* cell cycle in no-tumor hepatitis/cirrhosis by GRNInfer. Arrowhead represents activation relationship, empty cycle represents inhibition relationship. B: Candidate activated and inhibited upstream and downstream network of *BIRC5* cell cycle in HCC by GRNInfer. Arrowhead represents activation relationship, empty cycle represents inhibition relationship.

*UBE2C*, *CDC2* and inhibited *NEK2*, *CDC20*, *CDC6*, *MAPK3*, *CCNB1* in no-tumor hepatitis/cirrhosis. In order to further interpret molecular mechanism of *BIRC5* cell cycle module in no-tumor hepatitis/cirrhosis, we analyzed GO of the different activated and inhibited molecules from no-tumor hepatitis/cirrhosis. For example, activated *CCNA2* in no-tumor hepatitis/cirrhosis cellular component localized in female pronucleus, male pronucleus, nucleus, nucleoplasm, cytoplasm, and molecular function included protein binding, and biological process was relevant to cell cycle, mitosis, mitotic G2 checkpoint, positive regulation of transcription, cell division. Inhibited *CCNB1* in no-tumor hepatitis/cirrhosis cellular component localized in cellular component, nucleus, nucleoplasm, cytoplasm, centrosome, cytosol, and molecular function contained protein binding, and biological process was involved in G2/M

transition of mitotic cell cycle, cell cycle, mitosis, anaphase-promoting complex-dependent proteasomal ubiquitin-dependent protein catabolism, cell division, positive regulation of ubiquitin ligase activity during mitotic cell cycle. Our result demonstrated the different molecular network of *BIRC5* cell cycle module stronger nucleus protein binding but weaker cytoplasm protein binding as only characteristics in no-tumor hepatitis/cirrhosis. Therefore, we inferred *BIRC5* cell cycle module more mitosis but less complex-dependent proteasomal ubiquitin-dependent protein catabolism as a result increasing cell division and cell numbers in no-tumor hepatitis/cirrhosis.

Thirdly, we identified the different novel molecules of *BIRC5* cell cycle module in HCC compared with no-tumor hepatitis/cirrhosis. The different upstream *CCNE2*, *CCNA2*, *UBE2C*, *KATNB1* activated *BIRC5*, and *CDKN3*, *ZWINT*, *LLGL2*, *CCNB2*, *CCNB1*, *CDKN2C* inhibited *BIRC5*. The different downstream *BIRC5* activated *NEK2*, *CDC20*, *CDC6*, *MAPK3*, *CCNB1*, *KATNB1* and inhibited *CCNE2*, *ZWINT*, *LLGL2*, *UBE2C*, *CDC2* in HCC. In order to further interpret molecular mechanism of *BIRC5* cell cycle module in HCC, we analyzed GO of the different activated and inhibited molecules from HCC. For example, activated *NEK2* in HCC cellular component localized in nucleus, cytoplasm, centrosome, cytosol, protein complex, and molecular function included nucleotide binding, magnesium ion binding, protein serine/threonine kinase activity, protein binding, ATP binding, transferase activity, protein phosphatase binding, and biological process was relevant to cell cycle, regulation of mitosis, meiosis, protein amino acid autophosphorylation, centrosome separation, cell division. Inhibited *UBE2C* in HCC cellular component localized in nucleoplasm, cytosol, and molecular function comprised ubiquitin-protein ligase activity, ATP binding, ligase activity, and biological process was involved in ubiquitin-dependent protein catabolism, cell cycle, spindle organization and biogenesis, mitosis, cyclin catabolism, protein ubiquitination, anaphase-promoting complex-dependent proteasomal ubiquitin-dependent protein catabolism, positive regulation of exit from mitosis, phosphoinositide-mediated signaling, regulation of protein metabolism, cell division, negative regulation of ubiquitin ligase activity during mitotic cell cycle, positive regulation of ubiquitin ligase activity during mitotic cell cycle. Compared the same and different activated and inhibited *BIRC5* network with GO analysis, our result indicated the different molecular network of *BIRC5* cell cycle module stronger cytoplasm protein phosphatase binding but weaker ubiquitin-protein ligase activity as only characteristics in HCC. Therefore, we deduced *BIRC5* cell cycle module more protein amino acid autophosphorylation but less negative regulation of ubiquitin ligase activity during mitotic cell cycle as a result increasing growth and cell volume in HCC.

In conclusion, our high expression molecules of HCC did not contain *BIRC5* interaction proteins, whereas completely covered *BIRC5* pathway proteins by similarity comparison. We identified the same and different novel activated and inhibited upstream and downstream genes of *BIRC5* cell cycle module between no-tumor hepatitis/cirrhosis and HCC, on the condition that our *BIRC5* network covered *BIRC5* pathway and matched cell cycle enrichment analysis by the CapitalBio MAS 3.0 software from the published data. Our result showed *BIRC5* cell cycle network weaker transcription factor activity in both no-tumor hepatitis/cirrhosis and HCC (1); stronger nucleus protein binding but weaker cytoplasm protein binding in no-tumor hepatitis/cirrhosis (2); stronger cytoplasm protein phosphatase binding but weaker ubiquitin-protein ligase activity in HCC (3). We inferred *BIRC5* cell cycle module less transcription from RNA polymerase II promoter in both no-tumor hepatitis/cirrhosis and HCC (4). We deduced *BIRC5* cell cycle module different from more mitosis but less complex-dependent proteasomal ubiquitin-dependent protein catabolism as a result increasing cell division and cell numbers in no-tumor hepatitis/cirrhosis to more protein amino acid autophosphorylation but less negative regulation of ubiquitin ligase activity during mitotic cell cycle as a result increasing growth and cell volume in HCC (5). Therefore, it is very useful to identify *BIRC5* cell cycle network for the understanding of molecular mechanism between no-tumor hepatitis/cirrhosis and HCC transformation.

## ACKNOWLEDGMENTS

The Returned Overseas Chinese Scholars for Scientific research Foundation of State Education Ministry. Key philosophical and social science project of MOE (07JZD0005). Significant Science And Technology Project For New Transgenic Biological Species (2009ZX08012-001B). State Key Lab of Pattern Recognition Open Foundation.

## REFERENCES

Adhikari JS, Dwarakanath BS, Mathur R, Ravindranath T. 2003. Alterations in radiation induced cell cycle perturbations by 2-deoxy-D-glucose in human tumor cell lines. Indian J Exp Biol 41:1392–1399.

Andersen MH, Thor SP. 2002. Survivin—A universal tumor antigen. Histol Histopathol 17:669–675.

Aqui NA, Vonderheide RH. 2008. Survivin as a universal tumor antigen for novel cancer immunotherapy: Functions of a killer clone. Cancer Biol Ther 7:1888–1889.

Arlt D, Huber W, Liebel U, Schmidt C, Majety M, Sauermann M, Rosenfelder H, Bechtel S, Mehrle A, Bannasch D, Schupp I, Seiler M, Simpson JC, Hahne F, Moosmayer P, Ruschhaupt M, Guilleaume B, Wellenreuther R, Pepperkok R, Sultmann H, Poustka A, Wiemann S. 2005. Functional profiling: From microarrays via cell-based assays to novel tumor relevant modulators of the cell cycle. Cancer Res 65:7733–7742.

Braun K, Ehemann V, Waldeck W, Pipkorn R, Corban-Wilhelm H, Jenne J, Gissmann L, Debus J. 2004. HPV18 E6 and E7 genes affect cell cycle, pRB and p53 of cervical tumor cells and represent prominent candidates for intervention by use peptide nucleic acids (PNAs). Cancer Lett 209: 37–49.

Cheng T. 2004. Cell cycle inhibitors in normal and tumor stem cells. Oncogene 23:7256–7266.

Cheung AK, Lung HL, Hung SC, Law EW, Cheng Y, Yau WL, Bangarusamy DK, Miller LD, Liu ET, Shao JY, Kou CW, Chua D, Zabarovsky ER, Tsao SW, Stanbridge EJ, Lung ML. 2008. Functional analysis of a cell cycle-associated, tumor-suppressive gene, protein tyrosine phosphatase receptor type G, in nasopharyngeal carcinoma. Cancer Res 68:8137–8145.

Choudhury AD, Xu H, Baer R. 2004. Ubiquitination and proteasomal degradation of the BRCA1 tumor suppressor is regulated during cell cycle progression. J Biol Chem 279:33909–33918.

Dou QP, Smith DM, Daniel KG, Kazi A. 2003. Interruption of tumor cell cycle progression through proteasome inhibition: Implications for cancer therapy. Prog Cell Cycle Res 5:441–446.

Fey MF. 2000. [Cell cycle and cancer—From the tumor cell line to the patient]. Praxis (Bern 1994) 89:435–437.

Graf F, Koehler L, Kniess T, Wuest F, Mosch B, Pietzsch J. 2009. Cell cycle regulating kinase Cdk4 as a potential target for tumor cell treatment and tumor imaging. J Oncol 2009:106378.

Guha M, Altieri DC. 2009. Survivin as a global target of intrinsic tumor suppression networks. Cell Cycle 8:2708–2710.

Helt AM, Funk JO, Galloway DA. 2002. Inactivation of both the retinoblastoma tumor suppressor and p21 by the human papillomavirus type 16 E7 oncoprotein is necessary to inhibit cell cycle arrest in human epithelial cells. J Virol 76:10559–10568.

Hoshida Y, Villanueva A, Kobayashi M, Peix J, Chiang DY, Camargo A, Gupta S, Moore J, Wrobel MJ, Lerner J, Reich M, Chan JA, Glickman JN, Ikeda K, Hashimoto M, Watanabe G, Daidone MG, Roayaie S, Schwartz M, Thung S, Salvesen HB, Gabriel S, Mazzaferro V, Bruix J, Friedman SL, Kumada H, Llovet JM, Golub TR. 2008. Gene expression in fixed tissues and outcome in hepatocellular carcinoma. N Engl J Med 359:1995–2004.

Huang J, Wang L, Jiang M, Zheng X. 2010a. Interferon α-inducible protein 27 computational network construction and comparison between the frontal cortex of HIV encephalitis (HIVE) and HIVE-control patients. Open Genomics J 3:1–8.

Huang JX, Wang L, Jiang MH. 2010b. TNFRSF11B computational development network construction and analysis between frontal cortex of HIV encephalitis (HIVE) and HIVE-control patients. J Inflamm (Lond) 7:50.

Kim DY, Martin CB, Lee SN, Martin BK. 2005. Expression of complement protein C5a in a murine mammary cancer model: Tumor regression by interference with the cell cycle. Cancer Immunol Immunother 54:1026–1037.

Konduri S, Colon J, Baker CH, Safe S, Abbruzzese JL, Abudayyeh A, Basha MR, Abdelrahim M. 2009. Tolfenamic acid enhances pancreatic cancer cell and tumor response to radiation therapy by inhibiting survivin protein expression. Mol Cancer Ther 8:533–542.

Kuntzen C, Sonuc N, De Toni EN, Opelz C, Mucha SR, Gerbes AL, Eichhorst ST. 2005. Inhibition of c-Jun-*N*-terminal-kinase sensitizes tumor cells to CD95-induced apoptosis and induces G2/M cell cycle arrest. Cancer Res 65:6780–6788.

Liang QC, Xiong H, Zhao ZW, Jia D, Li WX, Qin HZ, Deng JP, Gao L, Zhang H, Gao GD. 2009. Inhibition of transcription factor STAT5b suppresses proliferation, induces G1 cell cycle arrest and reduces tumor cell invasion in human glioblastoma multiform cells. Cancer Lett 273:164–171.

Mhawech P, Greloz V, Oppikofer C, Szalay-Quinodoz I, Herrmann F. 2004. Expression of cell cycle proteins in T1a and T1b urothelial bladder carcinoma and their value in predicting tumor progression. Cancer 100:2367–2375.

Okada E, Murai Y, Matsui K, Isizawa S, Cheng C, Masuda M, Takano Y. 2001. Survivin expression in tumor cell nuclei is predictive of a favorable prognosis in gastric cancer patients. Cancer Lett 163:109–116.

Patino-Garcia A, Pineiro ES, Diez MZ, Iturriagagoitia LG, Klussmann FA, Ariznabarreta LS. 2003. Genetic and epigenetic alterations of the cell cycle regulators and tumor suppressor genes in pediatric osteosarcomas. J Pediatr Hematol Oncol 25:362–367.

Pham NA, Jacobberger JW, Schimmer AD, Cao P, Gronda M, Hedley DW. 2004. The dietary isothiocyanate sulforaphane targets pathways of apoptosis, cell cycle arrest, and oxidative stress in human pancreatic cancer cells and inhibits tumor growth in severe combined immunodeficient mice. Mol Cancer Ther 3:1239–1248.

Schoonjans K, Dubuquoy L, Mebis J, Fayard E, Wendling O, Haby C, Geboes K, Auwerx J. 2005. Liver receptor homolog 1 contributes to intestinal tumor formation through effects on cell cycle and inflammation. Proc Natl Acad Sci USA 102:2058–2062.

Schwartz TR, Vasta CA, Bauer TL, Parekh-Olmedo H, Kmiec EB. 2008. G-rich oligonucleotides alter cell cycle progression and induce apoptosis specifically in OE19 esophageal tumor cells. Oligonucleotides 18: 51–63.

Sotillo R, Renner O, Dubus P, Ruiz-Cabello J, Martin-Caballero J, Barbacid M, Carnero A, Malumbres M. 2005. Cooperation between Cdk4 and p27kip1 in tumor development: A preclinical model to evaluate cell cycle inhibitors with therapeutic activity. Cancer Res 65:3846–3852.

Stewart CJ, Crook ML, Leung YC, Platten M. 2009. Expression of cell cycle regulatory proteins in endometrial adenocarcinoma: Variations in conventional tumor areas and in microcystic, elongated and fragmented glands. Mod Pathol 22:725–733.

Storey JD. 2002. A direct approach to false discovery rates. J Roy Stat Soc, Ser B 64:479–498.

Sun Y, Lin R, Dai J, Jin D, Wang SQ. 2006. Suppression of tumor growth using antisense oligonucleotide against survivin in an orthotopic transplant model of human hepatocellular carcinoma in nude mice. Oligonucleotides 16:365–374.

Sun Y, Wang L, Lui L. 2008. Integrative decomposition procedure and Kappa statistics set up ATF2 ion binding module in Malignant Pleural Mesothelioma (MPM). Front Electr Electr Eng Chin 3:381–387.

Sun Y, Wang L, Jiang M, Huang J, Liu Z, Wolfl S. 2009. Secreted phosphoprotein 1 upstream invasive network construction and analysis of lung adenocarcinoma compared with human normal adjacent tissues by integrative biocomputation. Cell Biochem Biophys 56:59–71.

Turovets NA, Agapova LS, Kopnin PB, Tulina NM, Chumakov PM, Kopnin BP. 2000. [Effect of inactivating the p33ING1 tumor suppressor on the function of cell cycle ''checkpoints'' and genome stability]. Genetika 36: 385–392.

van der Veen AH, ten Hagen TL, Seynhaeve AL, Eggermont AM. 2002. Lack of cell-cycle specific effects of tumor necrosis factor-alpha on tumor cells in vitro: Implications for combination tumor therapy with doxorubicin. Cancer Invest 20:499–508.

Wang Y, Joshi T, Zhang XS, Xu D, Chen L. 2006. Inferring gene regulatory networks from multiple microarray datasets. Bioinformatics 22:2413–2420.

Wang L, Sun Y, Jiang M, Zhang S, Wolfl S. 2009a. FOS proliferating network construction in early colorectal cancer (CRC) based on integrative significant function cluster and inferring analysis. Cancer Invest 27:816–824.

Wang L, Sun Y, Jiang M, Zheng X. 2009b. Integrative decomposition procedure and Kappa statistics for the distinguished single molecular network construction and analysis. J Biomed Biotechnol 2009:726–728.

Wang L, Huang J, Jiang M. 2010a. CREB5 computational regulation network construction and analysis between frontal cortex of HIV encephalitis (HIVE) and HIVE-control patients. Cell Biochem Biophys [Epub ahead of print].

Wang L, Huang J, Jiang M. 2010b. RRM2 computational phosphoprotein network construction and analysis between no-tumor hepatitis/cirrhotic liver tissues and human hepatocellular carcinoma (HCC). Cell Physiol Biochem 26:303–310.

Wang L, Huang J, Jiang M, Sun L. 2010c. MYBPC1 computational phosphoprotein network construction and analysis between frontal cortex of HIV encephalitis (HIVE) and HIVE-control patients. Cell Mol Neurobiol [Epub ahead of print].

Wang L, Huang J, Jiang M, Zheng X. 2010d. AFP computational secreted network construction and analysis between human hepatocellular carcinoma (HCC) and no-tumor hepatitis/cirrhotic liver tissues. Tumour Biol 31:417–425.

Warrener R, Beamish H, Burgess A, Waterhouse NJ, Giles N, Fairlie D, Gabrielli B. 2003. Tumor cell-selective cytotoxicity by targeting cell cycle checkpoints. Faseb J 17:1550–1552.

Xia F, Canovas PM, Guadagno TM, Altieri DC. 2008. A survivin–ran complex regulates spindle formation in tumor cells. Mol Cell Biol 28:5299–5311.

Xiong H, Zhang ZG, Tian XQ, Sun DF, Liang QC, Zhang YJ, Lu R, Chen YX, Fang JY. 2008. Inhibition of JAK1, 2/STAT3 signaling induces apoptosis, cell cycle arrest, and reduces tumor cell invasion in colorectal cancer cells. Neoplasia 10:287–297.

Xu X, Qiao W, Linke SP, Cao L, Li WM, Furth PA, Harris CC, Deng CX. 2001. Genetic interactions between tumor suppressors Brca1 and p53 in apoptosis, cell cycle and tumorigenesis. Nat Genet 28:266–271.

Zolochevska O, Figueiredo ML. 2009. Expression of cell cycle regulator cdk2ap1 suppresses tumor cell phenotype by non-cell-autonomous mechanisms. Oral Oncol 45:e106–e112.